Crystals **2014**, *4*, 296-305; doi:10.3390/cryst4030296

OPEN ACCESS

crystals

ISSN 2073-4352

www.mdpi.com/journal/crystals

Article

Preparation and Characterization of Lead-Free $(K_{0.5}Na_{0.5})NbO_3$-$LiNbO_3$ and $(K_{0.5}Na_{0.5})NbO_3$-$LiTaO_3$ Ferroelectric Single Crystals

Tao Chu [1], Chao He [1], Hamel Tailor [2] and Xifa Long [1,*]

[1] Key Laboratory of Optoelectronic Materials Chemistry and Physics, Fujian Institute of Research on the Structure of Matter, Chinese Academy of Sciences, Fuzhou 350002, China; E-Mails: chutao@163.com (T.C.); hechao@fjirsm.ac.cn (C.H.)

[2] Department of Chemistry and 4D LABS, Simon Fraser University, Burnaby, BC V5A1S6, Canada; E-Mail: hntailor@sfu.ca

* Author to whom correspondence should be addressed; E-Mail: lxf@fjirsm.ac.cn; Tel.: +86-591-8371-0369.

Received: 20 April 2014; in revised form: 9 June 2014 / Accepted: 2 July 2014 / Published: 16 July 2014

Abstract: Lead-free $(K_{0.5}Na_{0.5})NbO_3$-$LiNbO_3$ (KNN-LN) and $(K_{0.5}Na_{0.5})NbO_3$-$LiTaO_3$ (KNN-LT) ferroelectric single crystals, with the dimensions of 11 × 11 × 5 mm^3 and 5 × 5 × 3 mm^3, were grown successfully using the top-seeded solution growth (TSSG) method, respectively. The crystal structures were analyzed by means of X-ray diffraction, showing orthorhombic symmetry for KNN-LN single crystals and coexistence of orthorhombic and tetragonal symmetry for KNN-LT single crystals at room temperature. The orthorhombic-tetragonal (T_{O-T}) and tetragonal-cubic (T_C) phase transition temperatures are 195 °C and 420 °C for the KNN-LN single crystals, and 130 °C and 280 °C for KNN-LT single crystals, respectively. The remnant polarization (P_r) is 27.8 μC/cm^2 with a coercive field (E_c) of 17 kV/cm for KNN-LT single crystals. The two single crystals showed 90° domains with layers in (parallel) straight lines, while KNN-LT single crystals have a larger domain region. The actual stoichiometry deviates easily from the original composition in the process of crystal growth, thus, an appropriate nominal composition and optimized crystal growth method is desired to get high-quality crystals in the future.

Keywords: crystal growth; lead-free ferroelectric materials; single crystals; domain

1. Introduction

Lead-based ferroelectric and piezoelectric materials, such as $PbTiO_3$-$PbZrO_3$ (PZT), are most widely used in acoustic transducers, solid actuators, and other electromechanical fields because of their high piezoelectric and electromechanical properties [1]. However, despite the toxic nature of PbO (which comprises 60–70 wt% of ceramic) it is most commonly used in PZT-based materials, therefore an urgent demand is to find lead-free materials to replace Pb-based ceramics in future. One of the most excellent candidates is potassium sodium niobate, $(K,Na)NbO_3$ (KNN), based solid solutions due to the high piezoelectric response, good ferroelectric properties, and especially high Curie temperature. Hollenstein *et al*. [2] prepared Li- and Ta-modified KNN-based ceramics, showing excellent properties with k_t of 52% and d_{33} over 300 pC/N. Saito *et al*. [3] synthesized textured $(K,Na,Li)(Nb,Ta,Sb)O_3$ ceramics with properties comparable to those of PZT ceramics (d_{33} > 300 pC/N, real permittivity > 1500, and planar coupling coefficient k_p > 60%). Guo *et al*. [4] prepared the $(1-x)$KNN-$x$$LiNbO_3$ ceramics, exhibiting excellent piezoelectric properties, d_{33} ~ 235 pC/N, k_t ~ 48%, and T_C ~ 460 °C, which is in the vicinity of the morphotropic phase boundary (MPB) of $(K_{0.5}Na_{0.5})NbO_3$ and $LiNbO_3$ binary solid solution system. In addition, some modified KNN ceramics prepared by conventional solid-state sintering method have been investigated [5–8].

Compared with KNN-based ceramic, KNN-based single crystals have more excellent piezoelectric properties, as demonstrated in many materials, such as $0.95(K_{0.5}Na_{0.5})NbO_3$-$0.05LiNbO_3$ and $Bi_{0.5}Na_{0.5}TiO_3$-$BaTiO_3$ lead-free single crystals [9,10]. Some other KNN-based single crystals have been reported in recent years, for example, Yoichi *et al*. [10] presented the control of defect for low leakage current in KNN and Mn-KNN single crystals, grown by a self-flux method. A high thickness-coupling coefficient in $[001]_c$-oriented $Li_{0.02}(Na_{0.5}K_{0.5})_{0.98}NbO_3$ single crystals was obtained using top-seeded solution growth [11].

The aim of our work is to study the crystal structure, dielectric properties, and domain configuration of $(K_{0.5}Na_{0.5})NbO_3$-$LiNbO_3$ (KNN-LN) and $(K_{0.5}Na_{0.5})NbO_3$-(KNN-LT) single crystals grown by the top-seeded solution growth (TSSG) method.

2. Results and Discussion

2.1. Structural and Compositional Analysis

At the end of the TSSG growth, the KNN-LN and KNN-LT single crystals with dimensions of $11 \times 11 \times 5$ mm^3 and $5 \times 5 \times 3$ mm^3 were obtained, as shown in Figure 1. Inductively coupled plasma atomic emission spectroscopy (ICP-AES) was used to analysis the components of obtained crystals, which were found to easily deviate from the original composition. The compositional deviation is listed in Table 1. One reason is the high volatility of potassium and sodium, another one is the large difference of ionic radii: K^+ (1.38 Å), Na^+ (1.02 Å) and Li^+ (0.76 Å), making it more difficult for K^+ and Li^+ to enter the cell during crystal growth. Figure 2 presents the X-ray diffraction (XRD) patterns measured at room temperature. It can be seen that the KNN-LN and KNN-LT single crystals are of pure perovskite phase. Special attention was focused on (200)/(020) reflections around $2\theta = 45°$ in order to study the detailed structure. For an orthorhombic symmetry with $a = c > b$, its I(200)/I(020) equals 2 and the (200) line has a low Bragg angle. But the I(002)/I(200) equals 0.5 and the (002) line is located at a low Bragg

angle for tetragonal symmetry $a = b < c$ [12]. It should be noted that the primitive unit cell of the orthorhombic perovskite structure is actually of monoclinic symmetry, as there is an angle β slightly larger than 90° [13,14]. Based on the above analysis, it is found that the KNN-LN single crystals have pure orthorhombic phase, and the KNN-LT single crystals have orthorhombic and tetragonal phase simultaneously at room temperature. The intensity ratio of orthorhombic to tetragonal for KNN-LT single crystals equals 2.5. The lattice parameters of the grown single crystals were calculated based on XRD data at room temperature. The corresponding values (*a*, *b*, *c*) are listed in Table 1.

Figure 1. Photograph of (**a**) $(K_{0.5}Na_{0.5})NbO_3$-$LiNbO_3$ and (**b**) $(K_{0.5}Na_{0.5})NbO_3$-$LiTaO_3$ single crystals grown by the top-seeded solution growth (TSSG) method.

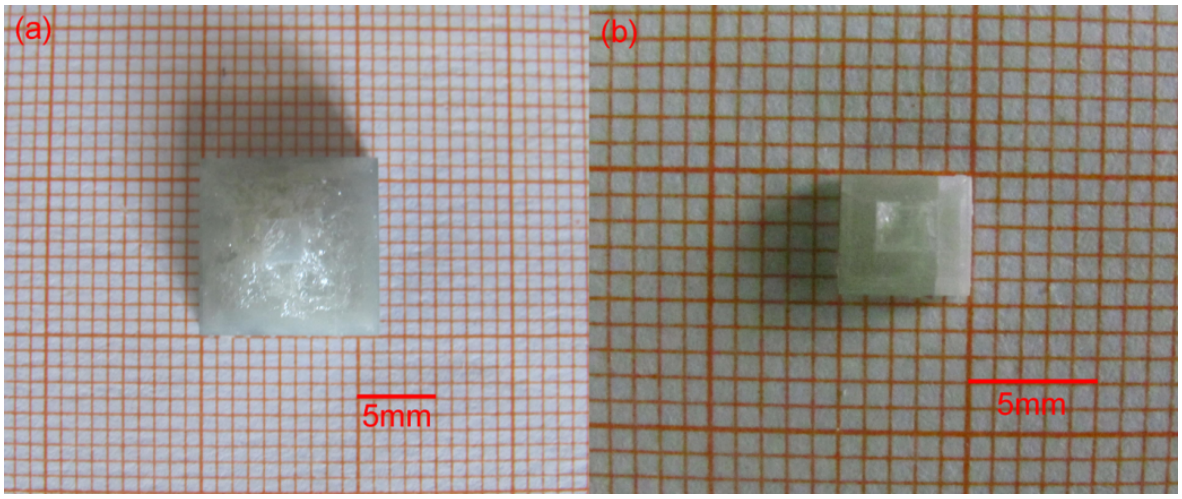

Figure 2. (**a**) X-ray diffraction patterns of KNN-LN and KNN-LT single crystals and (**b**) $(200)_c$ diffraction peak.

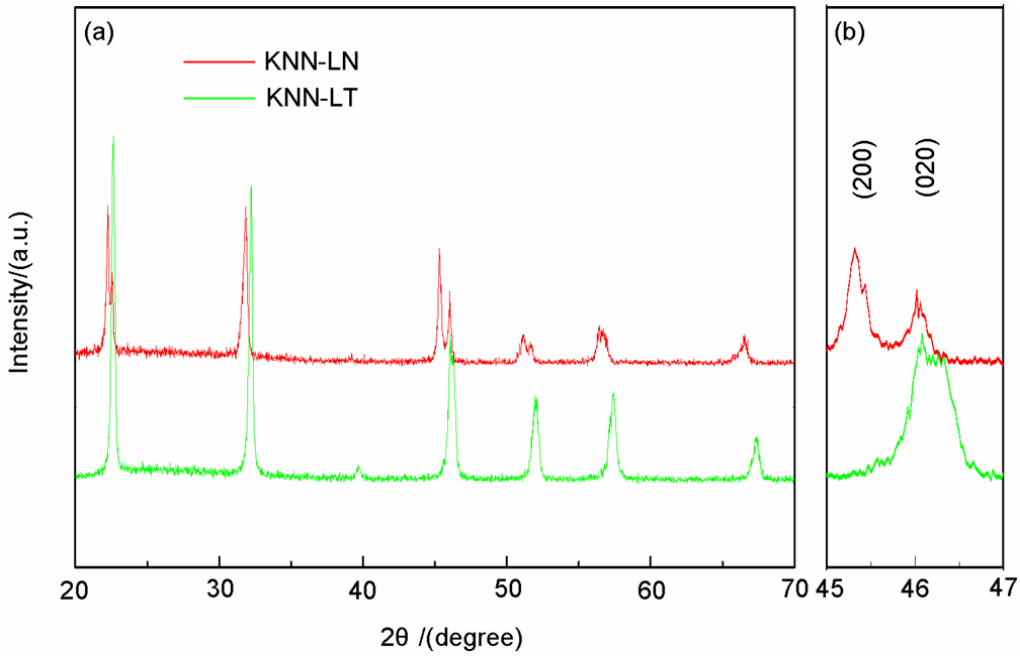

Table 1. Actual composition and physical parameters of $(K_{0.5}Na_{0.5})NbO_3$-$LiNbO_3$ (KNN-LN) and $(K_{0.5}Na_{0.5})NbO_3$-$LiTaO_3$ (KNN-LT) single crystals.

Parameters	KNN-LN	KNN-LT
Original composition	K/Na/Li (64.37/25.76/9.87)	K/Na/Li, Nb/Ta (48.42/48.42/3.16, 94/6)
Actual composition	(49.00/50.60/0.40)	(22.72/77.07/0.21, 77.45/22.55)
a (+/−0.001)	4.000	3.932
b (+/−0.001)	3.938	3.922
c (+/−0.001)	3.991	3.924
T_C (°C) (+/−1 °C)	420	280
$T_{O\text{-}T}$ (°C) (+/−1 °C)	195	130
ε_r (@ 30 °C) (+/−0.1)	535	254
tanδ (@ 30 °C) (+/−0.01)	0.06	0.14

2.2. Dielectric Properties

The temperature dependence of real permittivity (ε_r) and dielectric loss tangent (tanδ) for unpoled KNN-LN and KNN-LT single crystals as a function of temperature at frequencies of 100 kHz and 1 MHz were shown in Figure 3. There are two peaks are observed at 195 °C and 420 °C for KNN-LN single crystals, and 130 °C and 280 °C for KNN-LT single crystals corresponding to the orthorhombic-tetragonal phase transition temperature ($T_{O\text{-}T}$) and the tetragonal-cubic phase transition temperature T_C, respectively. For the two phase transition temperature, the KNN-LN single crystals is approximately consistent with KNN-0.05LN single crystals [1] and the T_C of KNN-LT single crystals decreases to 280 °C, compared with KNN, due to the addition of Ta content. However, the Curie point over 310 °C of $(K_{0.485}Na_{0.485}Li_{0.3})(Nb_{0.8}Ta_{0.2})O_3$ ceramics is due to the addition of Li [2]. It is worth noting that real permittivity of KNN-LN single crystals is higher than KNN-LT single crystals at room temperature, but the results is contrast at the temperature of T_C. In the high temperature region, the high value of ε_r may be attribute to the contributions from space charge polarization, which comes from mobility of ions and imperfections in the material [15,16]. It shows that KNN-LT single crystals' quality is worse than KNN-LN single crystals, the results can also be derived from the dielectric loss spectrum in Figure 3.

Figure 3. Real permittivity and loss tangent of (**a**) KNN-LN and (**b**) KNN-LT single crystals as a function of temperature at 100 kHz and 1 MHz.

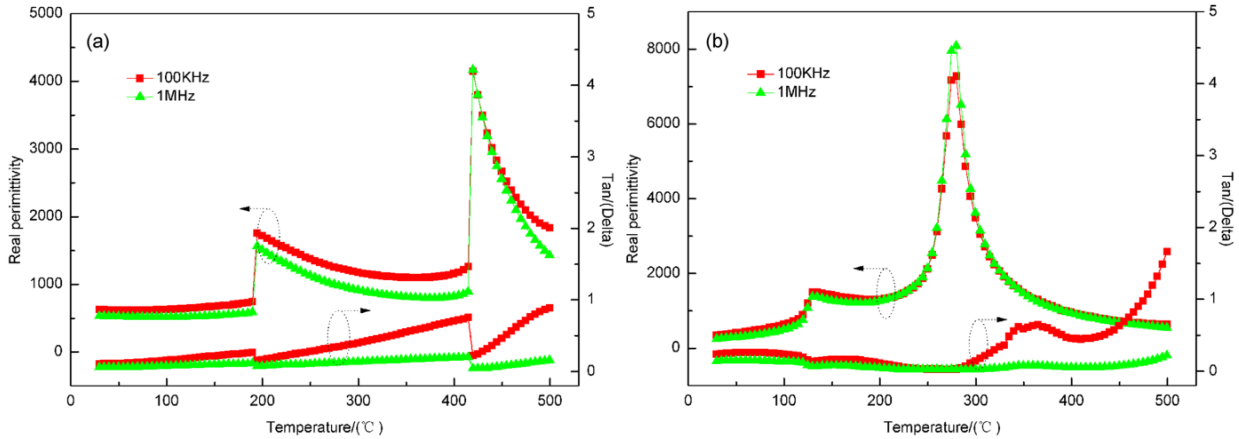

As shown in Figure 3, tanδ decrease above $T_{O\text{-}T}$ and increased again above T_C. Dielectric loss increases rapidly because of the ionic conduction and the movement of oxygen and potassium vacancies at the high temperature [1,15]. The vacancies arise because the crystals were grown in the air and potassium oxide volatilizes at the high temperature, it will lead to the existence of leading vacancies in the grown crystals. Similar phenomenon has been discovered in some other perovskite structure systems, such as $Pb(Fe_{1/2}Nb_{1/2})O_3$-$Pb(Yb_{1/2}Nb_{1/2})O_3$-$PbTiO_3$ single crystals and KNN ceramics [16,17].

2.3. Ferroelectric Properties and Domain Configuration

The ferroelectric hysteresis loops for [100]-oriented KNN-LT single crystals (at 20 Hz) are shown in Figure 4. The coercive electric field (E_c) and the remanent polarization (P_r) were 17 kV/cm and 27.8 μC/cm^2, respectively. The KNN-LN single crystal does not show a typical ferroelectric hysteresis loops because of the high level of leakage current induced by oxide vacancies, which is in good agreement with the loop of KNN-0.05LN single crystals [1].

Figure 4. *P–E* hysteresis loops of KNN-LT single crystals at 20 Hz.

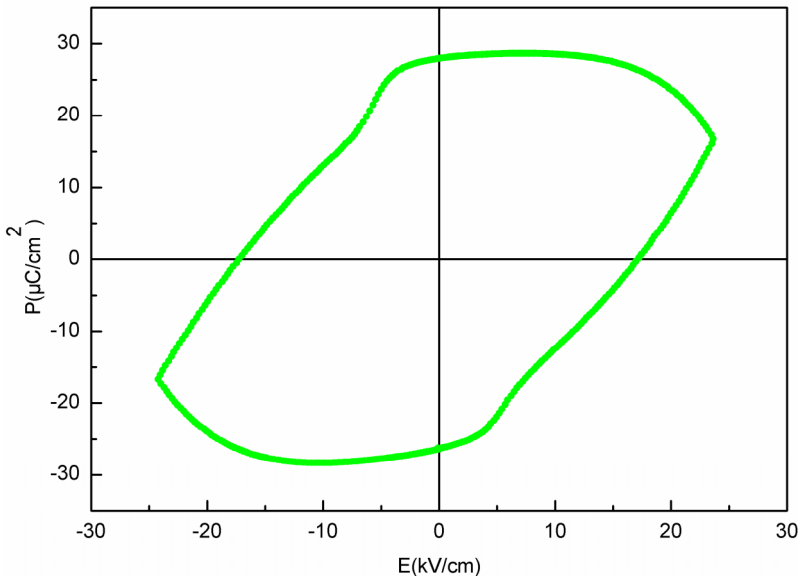

The ferroelectric and piezoelectric is determined by the polarization response under external and low external mechanical stress. So, the study of domain in KNN-LN and KNN-LT single crystals is critical for a better understanding of their properties. In the past years, a few papers dealing with the ferroelectric domains in KNN-based materials are reported in the literature [18,19]. Fu *et al*. [19] investigated the composition-dependent domain morphology of $(Na_{0.52}K_{0.48-x})(Nb_{0.92-x}Sb_{0.08})O_3$-$x$LiTaO$_3$ ceramics by means of transmission electron microscopy (TEM). Nanodomains of alternate orthorhombic and tetragonal domains with a width of 20–50 nm were observed near polymorphic phase coexistence zone [19]. Rubio-Marcos *et al*. [18] presented and discussed the spatial resolved structure of the ferroelectric domain existing in (K,Na)NbO$_3$ based ceramics studied by confocal Raman microscopy (CRM) coupled with atomic force microscopy. In this work, we presented domain configuration using a polarized light microscope. Under a crossed polarizer, the sample appears to be in extinction where the vibration directions of the polarizer and analyzer are directed along the slow and fast vibration directions

of the domain. So, the domain structure can be determined according to the extinction positions. Domain patterns of [001]-oriented unpoled KNN-LN and KNN-LT single crystals are displayed in Figure 5. A laminar domain structure of KNN-LN single crystals in which domain wall lies along the [100] direction are observed at room temperature, belonging to 90° domains, as shown in Figure 5a. It is some different from the domains of KNN single crystals, which are zig-zag shaped 90° domains but similar with the domains width (0.7 μm) of KNN single crystals [20]. When we observe the [001]-oriented of KNN-LN and KNN-LT single crystals in crossed polarizer, the extinction directions parallel to [100] for tetragonal domain (90° domains) while orthorhombic phase will generate domains with extinction parallel to [110], 45° rotate from [100] direction. Figure 5b also demonstrated that the single crystals are orthorhombic structure according to the extinction directions parallel to [110] after Figure 5a rotated 45°. There was also a laminar domain structure of KNN-LT single crystals whose domain width from 1.25 to 11.8 μm, which was larger than that of KNN-LN single crystals, as shown in Figure 5c. The KNN-LT single crystal is of orthorhombic symmetry in the area of Figure 5c,d. Generally, Ta should be substituted for B-site of the perovskite-type structure; therefore, the substitution of Ta can change the shape of the BO_6 unit in perovskite-type structure and the internal stress in the crystal. As Mn substitution can significantly release the inter stress, Ta can also release the inter stress, leading to larger domain area than KNN-LN single crystals [20].

Figure 5. Domain patterns of [001]-oriented single crystals under crossed polarizer at room temperature: (**a**) and (**b**) for KNN-LN; (**c**) and (**d**) for KNN-LT.

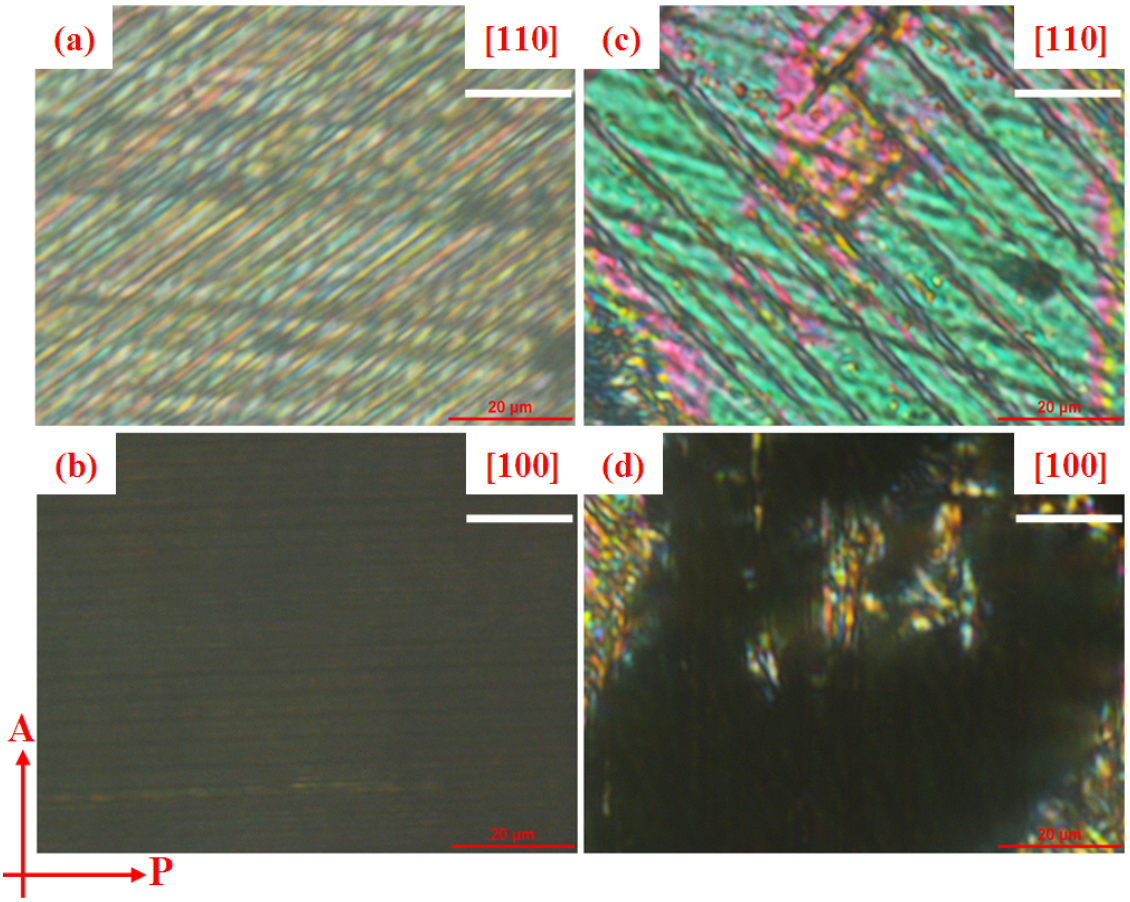

Figure 6 shows the orthorhombic and tetragonal coexisted in KNN-LT single crystals at room temperature under crossed polarizer. The crystals presented two types of structures, one tetragonal with extinctions along [100] direction, as shown in the region marked as 1 which is the representative of the black regions in Figure 6a, the other orthorhombic with extinctions along [110] direction, as shown in the region marked as 2 which displays the bright regions in Figure 6a. Figure 6b shows the phenomenon of optical change after Figure 6a rotated 45° under crossed polarizer. The dark areas became bright and bright areas became dark demonstrated the orthorhombic and tetragonal coexisted in the KNN-LT single crystals.

Figure 6. Domain structure of [001]-oriented KNN-LT single crystals, (**a**) [110] and (**b**) [100] parallel to polarizer.

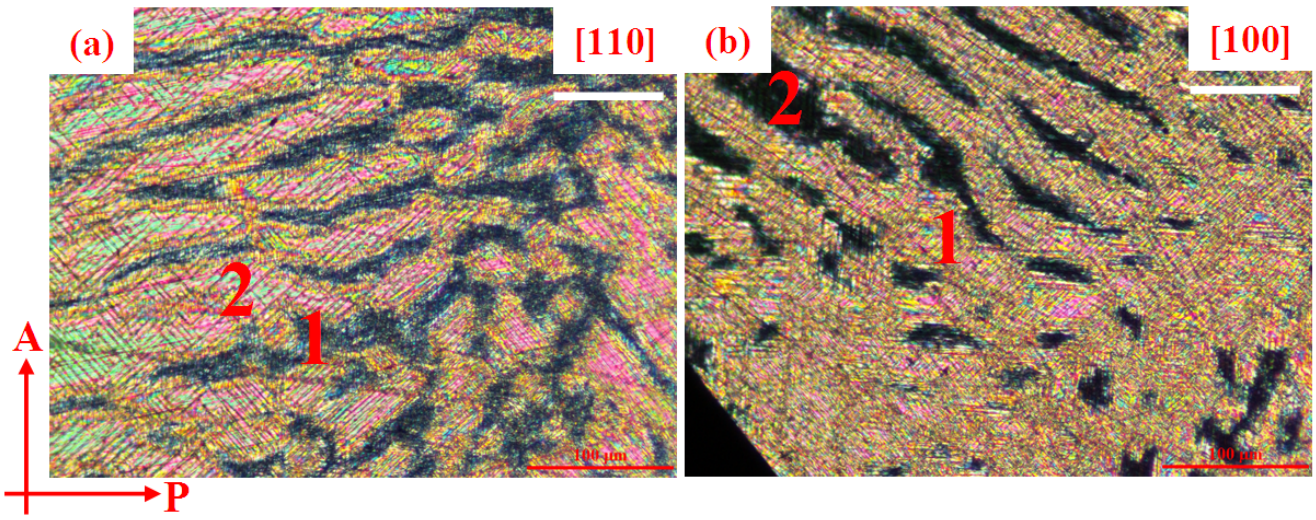

3. Experimental Section

3.1. Crystal Growth

The KNN-LN and KNN-LT single crystals were grown by the TSSG method. The starting chemicals, K_2CO_3 (99.99%), Na_2CO_3 (99.90%,), Li_2CO_3 (99.99%), Nb_2O_5 (99.90%), Ta_2O_5 (99.99%) (Sinopharm Chemical Reagent Co., Ltd, Shanghai, China) were weighed according to the designed solute composition of $(K_{0.5}Na_{0.5})NbO_3$-$LiNbO_3$ and $(K_{0.5}Na_{0.5})NbO_3$-$LiTaO_3$. A mixture of K_2CO_3, Na_2CO_3 and Li_2CO_3 was used as high temperature solution to reduce the crystallization temperature and compensate for the deviation of the composition due to the segregation of K and Li. The mixture was placed in a platinum crucible, which was then placed into a vertical tubular furnace to melt. The used KNN-LN and KNN-LT seed crystals were obtained from preliminary flux growth method. The saturation temperature (T_s), *i.e.*, crystallization temperature, of the solution was determined to be about 850–1000 °C by repeated seeding trials. The T_s changed due to the change of solution and temperature distribution in furnace in each crystals growth process. At the stage of growth, the slow cooling rate was set from 0.05 to 0.10 °C/h. The growing crystal was rotated at a speed of 0–30 rpm. At the end of growth process, the grown crystal was pulled out of the melt surface and then cooled down to room temperature at a rate of 20 °C/h. KNN-LN and KNN-LT single crystals were obtained at the end of the growths.

3.2. Characterization Procedures

The structural analysis was performed by means of X-ray diffraction (XRD) technical. The powder sample was pulverized from a small fraction of the obtained crystals. The XRD data were collected at room temperature on a Rigaku Diffractometer (Rigaku Corporation, Tokyo, Japan) equipped with Cu Kα radiation and a graphite monochromator, with scanning steps of 0.02° (2θ) and an angular range of 20°–70°. The actual chemical composition of the grown crystals is analyzed by inductively coupled plasma-atomic emission spectroscopy (ICP-AES, Ultima-2, Jobin Yvon, Paris, France). For the symmetry of the obtained crystals and domain configuration characterization, sheet samples were prepared. The sheet samples were cut from the obtained single crystals according to a certain direction. The cut sheet samples were cemented on a copper mold with paraffin, and the two surfaces polished with different grit sandpapers into a thickness of about 50 μm. The samples were observed by a polarized light microscope (LV100POL, Nikon, Tokyo, Japan). For electric characterization, different shapes of plates along [001] direction were sliced from the obtained crystals, and then the samples were polished and coated with silver paste as electrodes. For dielectric, ferroelectric and piezoelectric measurements, the thickness of plate samples was about 0.5 mm. The dielectric constant (ε_r) and dielectric loss tangent (tanδ) were measured at various frequencies as a function of temperature upon heating from 30 to 500 °C using a Novocontrol broadband dielectric spectrometer (Novocontrol GmbH, Montabaur, Germany), with an AC signal Amplitude of 1 V (peak-to-peak) applied. Ferroelectric hysteresis loops were displayed by aix-ACCT TF Analyzer 2000 standard ferroelectric test system (aixACCT Systems GmbH, Aachen, Germany) at f = 20 Hz combined with a high-voltage amplifier (Model 610E, Trek, Lockport, NY, USA) at room temperature.

4. Conclusions

KNN-LN and KNN-LT ferroelectric single crystals were successfully grown by TSSG method. The KNN-LN single crystals are of orthorhombic symmetry and KNN-LT single crystals display the coexistence of orthorhombic and tetragonal regions at room temperature. It was found that, Ta^{5+} doping reduces the tetragonal-cubic phase transition temperature from 420 to 280 °C and the orthorhombic-tetragonal phase translation temperature from 195 to 130 °C. The dielectric loss increases rapidly above T_C because of the effect of potassium and oxygen vacancies. The ferroelectric hysteresis loops of KNN-LT single crystals are round shaped and not saturated, suggesting the large leakage current induced by oxide vacancies. Additionally, the Ta doping can release the inter-unit cell stress, and lead to larger domain size than KNN-LN single crystals. In future work, improving the TSSG method will be performed with a focus on potential applications.

Acknowledgments

This work was supported by the National Natural Science Foundation of China (Grant No. 91122020) and the Youth Innovation Funding of Fujian Province (2014J05069).

Author Contributions

Tao Chu contributed to the experiment, the data analyses and manuscript preparation. Chao He contributed to analysis and manuscript preparation. Hamel Tailor performed the manuscript preparation. Xifa Long conceived and designed the study.

Conflicts of Interest

The authors declare no conflict of interest.

References

1. Chen, K.; Xu, G.S.; Yang, D.F.; Wang, X.F.; Li, J.B. Dielectric and piezoelectric properties of lead-free $0.95(K_{0.5}Na_{0.5})NbO_3$-$0.05LiNbO_3$ crystals grown by the Bridgman method. *J. Appl. Phys.* **2007**, *101*, 044103:1–044103:4.
2. Hollenstein, E.; Davis, M.; Damjanovic, D.; Setter, N. Piezoelectric properties of Li- and Ta-modified$(K_{0.5}Na_{0.5})NbO_3$ ceramics. *Appl. Phys. Lett.* **2005**, *87*, 182905:1–182905:3.
3. Saito, Y.; Takao, H.; Tani, T.; Nonoyama, T.; Takatori, K.; Homma, T.; Nagaya, T.; Nakamura, M. Lead-free piezoceramics. *Nature* **2004**, *432*, 84–87.
4. Guo, Y.P.; Kakimoto, K.; Ohsato, H. Phase transitional behavior and piezoelectric properties of $(Na_{0.5}K_{0.5})NbO_3$-$LiNbO_3$ ceramics. *Appl. Phys. Lett.* **2004**, *85*, 4121–4123.
5. Meng, H.Q.; Yang, Y.; Wang, Y.P.; Wan, D.D.; Li, Q.; Cheng, Y. Alkaline earth elements modified lead-free $0.96(K_{0.5}Na_{0.5})NbO_3$-$0.04LiTaO_3$ ceramics. *Ferroelectrics* **2010**, *404*, 105–111.
6. Matsubara, M.; Yamaguchi, T.; Sakamoto, W.; Kikuta, K.; Yogo, T.; Hirano, S. Processing and piezoelectric properties of lead-free $(K,Na)(Nb,Ta)O_3$ ceramics. *J. Am. Ceram. Soc.* **2005**, *88*, 1190–1196.
7. Rubio-Marcos, F.; Ochoa, P.; Fernandez, J.F. Sintering and properties of lead-free $(K,Na,Li)(Nb,Ta,Sb)O_3$ ceramics. *J. Eur. Ceram. Soc.* **2007**, *27*, 4125–4129.
8. Rubio-Marcos, F.; Marchet, P.; Merle-Méjean, T.; Fernandez, J.F. Role of sintering time, crystalline phases and symmetry in the piezoelectric propereties of lead-free KNN-modified ceramics. *Mater. Chem. Phys.* **2010**, *123*, 91–97.
9. Chen, C.; Jiang, X.P.; Li, Y.M.; Wang, F.F.; Zhang, Q.H.; Luo, H.S. Growth and electrical properties of $Na_{1/2}Bi_{1/2}TiO_3$-$BaTiO_3$ lead-free single crystal with morphotropic phase boundary composition. *J. Appl. Phys.* **2010**, *108*, 124106:1–124106:5.
10. Kizaki, Y.; Noguchi, Y.; Miyayama, M. Defect control for low leakage current in$K_{0.5}Na_{0.5}NbO_3$ single crystals. *Appl. Phys. Lett.* **2006**, *89*, 142910:1–142910:3.
11. Davis, M.; Klein, N.; Damjanovic, D.; Setter, N.; Gross, A.; Wesemann, V.; Vernay, S.; Rytz, D. Large and stable thickness coupling coefficients of $[001]_c$-oriented $KNbO_3$ and Li-modified $(K,Na)NbO_3$ single crystals. *Appl. Phys. Lett.* **2007**, *90*, 062904:1–062904:3.
12. Zhou, J.J.; Li, J.F.; Wang, K.; Zhang, X.W. Phase structure and electrical properties of (Li,Ta)-doped $(K,Na)NbO_3$ lead-free piezoceramics in the vicinity of Na/K = 50/50. *J. Mater. Sci.* **2011**, *46*, 5111–5116.

13. Wang, K.; Li, J.F. Domain engineering of lead-free Li-modified (K,Na)NbO_3 polycrystals with highly enhanced piezoelectricity. *Adv. Funct. Mater.* **2010**, *20*, 1924–1929.
14. Tellier, J.; Malic, B.; Dkhil, B.; Jenko, D.; Cilensek, J.; Kosec, M. Crystal structure and phase transitions of sodium potassium niobate perovskites. *Solid State Sci.* **2009**, *11*, 320–324.
15. Lin, D.B.; Li, Z.R.; Zhang, S.J.; Xu, Z.; Yao, X. Dielectric/piezoelectric properties and temperature dependence of domain structure evolution in lead free $Na_{0.5}K_{0.5}NbO_3$ single crystal. *Solid State Commun.* **2009**, *149*, 1646–1649.
16. Kumar, P.; Pattanaik, M.; Sonia. Synthesis and characterizations of KNN ferroelectric ceramics near 50/50 MPB. *Ceram. Int.* **2013**, *39*, 65–69.
17. He, C.; Li, X.Z.; Wang, Z.J.; Liu, Y.; Shen, D.Q.; Li, T.; Long, X.F.; Ye, Z.G. Growth of $Pb(Fe_{1/2}Nb_{1/2})O_3$-$Pb(Yb_{1/2}Nb_{1/2})O_3$-$PbTiO_3$ piezo-/ferroelectric crystals for high power and high temperature applications. *CrystEngComm* **2012**, *14*, 4407–4413.
18. Rubio-Marcos, F.; Campo, A.D.; López-Juárez, R.; Romero, J.J.; Fernández, J.F. High spatial resolution structure of (K,Na)NbO_3 lead-free ferroelectric domains. *J. Mater. Chem.* **2012**, *22*, 9714–9720.
19. Fu, J.; Zuo, R.; Xu, Z. High piezoelectric activity in (Na,K)NbO_3 based lead-free piezoelectric ceramics: Contribution of nanodomains. *Appl. Phys. Lett.* **2011**, *99*, 062901:1–062901:3.
20. Inagaki, Y.; Kakimoto, K.; Kagomiya, I. Crystal growth and ferroelectric property of $Na_{0.5}K_{0.5}NbO_3$ and Mn-doped $Na_{0.5}K_{0.5}NbO_3$ crystals grown by floating zone method. *J. Eur. Ceram. Soc.* **2010**, *30*, 301–306.